

PHYS4070 Assignment 1

Ryan White

26th of March 2024

Introduction

Modelling the hydrogen atom is relatively straight forward process that utilises fundamental atomic physics. The same physics does not necessarily describe more complex quantum systems that host more electrons such as in the lithium atom. Herein we investigate several approximate treatments for lithium atomic physics using the modified potential function,

$$V(r) = -\frac{Z}{r} + \frac{l(l+1)}{2r^2} + V_{e-e} \quad (1)$$

as a starting point.

B1 - Hydrogen-like lithium

As a warm up, we simplified the matrix elements under the spherically symmetric (i.e. radial) assumption, writing our final result in terms of the separable radial wave function $P(\mathbf{r})$,

$$\langle nlm|r|n'l'm'\rangle = \int \psi_{nlm}^\dagger(\mathbf{r}) r \psi_{n'l'm'}(\mathbf{r}) r^2 \sin \theta dr d\theta d\phi \quad (2)$$

$$= \int \frac{P_{nl}(r)}{r} \cdot r \cdot \frac{P_{n'l'}(r)}{r} \cdot r^2 \cdot Y_{lm}^\dagger(\theta, \phi) \cdot Y_{l'm'}(\theta, \phi) \sin \theta dr d\theta d\phi \quad (3)$$

$$= \int P_{nl}(r) \cdot r \cdot P_{n'l'}(r) \cdot \delta_{ll'} \delta_{mm'} dr \quad (4)$$

$$= \delta_{ll'} \delta_{mm'} \int P_{nl}(r) \cdot r \cdot P_{n'l'}(r) dr \quad (5)$$

Here we've used that $\psi_{nlm}(\mathbf{r}) = (P_{nl}(r) Y_{lm}(\theta, \phi))/r$, i.e. that the wavefunction is separable for a radial probability and an angular spherical harmonic component. We've also used that

$$\int Y_{lm}^\dagger Y_{l'm'} d\Omega = \delta_{ll'} \delta_{mm'} \quad (6)$$

to reduce the angular component of the wavefunction (where $d\theta d\phi$ subtends the solid angle $d\Omega$). Equation (6) essentially enforces that only like spherical harmonics will result in a non-zero matrix element.

To begin the numerical investigation for the hydrogen-like lithium problem, we constructed a 47×47 Hamiltonian matrix where each element was constructed as in the equation

$$H_{ij} = \frac{1}{2} \int b'_i(r) b'_j(r) dr + \int b_i(r) V(r) b_j(r) dr \quad (7)$$

from Worksheet 2, and a 47×47 B-spline basis matrix as in equation (10) of the assignment sheet. Numerical integration was performed with the trapezoidal rule over a grid of 2000 points from $r_0 = 10^{-5}$ au to $r_{\max} = 50$ au. Our B-splines were calculated using the supplied code `bspline.hpp`, with our choosing of $N = 50$ 7th order B-splines and the same radial coordinates as the integration grid. To enforce the boundary conditions, we ignored the first two and last one B-spline (hence our $N - 3$ dimension Hamiltonian and basis matrices).

Using the LAPACK linear algebra solver `dsygv_()`, we solved the Schrodinger equation with the hydrogen-like lithium potential for the problem $H\mathbf{c} = \varepsilon B\mathbf{c}$. The hydrogen-like lithium potential is described as

$$V(r) = -\frac{Z}{r} + \frac{l(l+1)}{2r^2} \quad (8)$$

i.e. by setting $V_{e-e} = 0$ in equation (1). We show our obtained eigenstates, along with our radial wavefunction expectation value in Table 1.

n	s ($l = 0$) States				p ($l = 1$) States			
	E_n (calc)	E_n (analytic)	$\langle r \rangle_{\text{calc}}$	$\langle r \rangle_{\text{analytic}}$	E_n (calc)	E_n (analytic)	$\langle r \rangle_{\text{calc}}$	$\langle r \rangle_{\text{analytic}}$
1	-4.479	-4.5	0.502	0.500	-	-	-	-
2	-1.122	-1.125	2.005	2.000	-1.125	-1.125	1.667	1.667
3	-0.499	-0.500	4.507	4.500	-0.500	-0.500	4.167	4.167
4	-0.281	-0.281	8.010	8.000	-0.281	-0.281	7.667	7.667
5	-0.180	-0.180	12.512	12.500	-0.180	-0.180	12.167	12.167
6	-0.125	-0.125	18.015	18.000	-0.125	-0.125	17.667	17.667
7	-0.092	-0.092	24.495	24.500	-0.092	-0.092	24.148	24.167
8	-0.070	-0.070	30.628	32.000	-0.070	-0.070	30.382	31.667
9	-0.049	-0.055	31.867	40.500	-0.050	-0.055	31.782	40.167
10	-0.024	-0.045	30.690	50.000	-0.025	-0.045	30.609	49.667

Table 1 Energies and expectation values for first 10 s and p states of hydrogen-like lithium. The analytic values for energy and expectation value were calculated from equations (12) and (13) in the assignment task sheet. All values are quoted in atomic units.

We see excellent agreement ($\ll 1\%$) between our results and the analytic eigenstates/expectation values up to about $n \sim 8$. Around this point, the expectation values become close to our chosen maximum in the numerical integration grid ($r = 50\text{au}$), and so our radial wavefunction is no longer $P(r) = 0$ at the grid boundary. That is, we numerically truncate our function at $r = 50\text{au}$ when this is no longer a valid approximation for the high energy states whose wavefunction extends past this value.

Our radial probability densities for the first 2 s and first p states are shown in Figure 1.

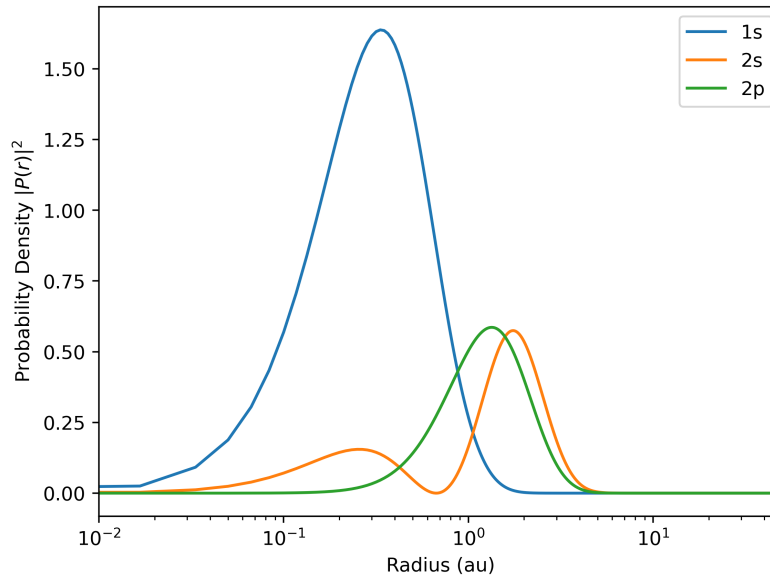


Figure. 1 Radial probability densities for the 1s and two first valence states, 2s and 2p, of hydrogen-like lithium.

B2 - Neutral lithium: Green's approximation

The Green's approximation inputs the Green's potential into our radial Hamiltonian,

$$V_{e-e}(r) \approx V_{\text{Gr}}(r) = \frac{(Z-1)}{r} \frac{h(e^{r/d} - 1)}{1 + h(e^{r/d} - 1)} \quad (9)$$

which emulates the electron-electron repulsion – a first step in the many-body quantum problem that distances our treatment of lithium from a hydrogen-like approximation. For lithium, we take $h = 1$ and $d = 0.2$, and substitute this into our potential function which is used to populate the Hamilton matrix elements (equation 7). With this modification made, the process of solving the Schrodinger equation is the same as in section B1.

We're given that the experimental values for binding energy of the lowest two valence states is $\varepsilon_{2s}^{\text{Expt.}} \approx -0.19814\text{au}$ and $\varepsilon_{2p}^{\text{Expt.}} \approx -0.13023\text{au}$. With the modifications made using Green's potential, we get the binding energies $\varepsilon_{2s} = -0.15582\text{au}$ and $\varepsilon_{2p} = -0.12541\text{au}$, corresponding to errors of $\sim 21.36\%$ and $\sim 3.70\%$ respectively. The corresponding radial probability densities using Green's approximation are shown in Figure 2. The main differences between this and the hydrogen-like treatment is that the probability peaks are shifted to higher radius with lower peak values.

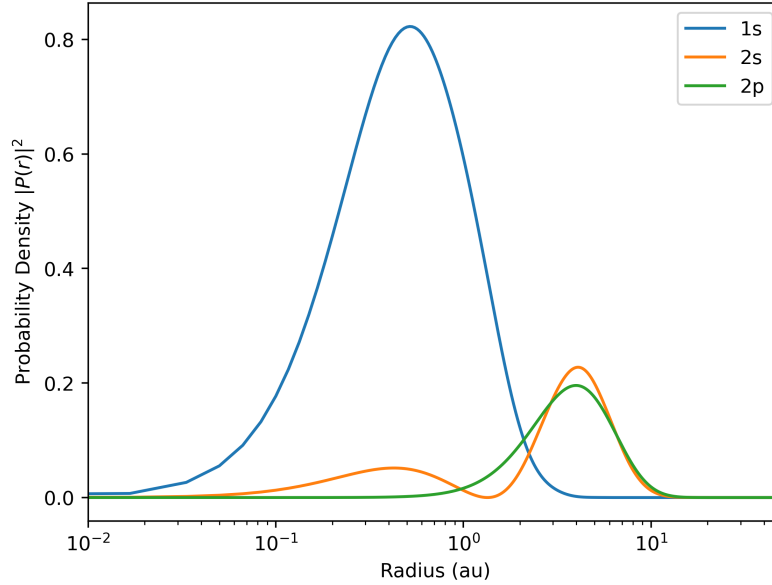


Figure. 2 Radial probability densities for the 1s and two first valence states, 2s and 2p, using the Green's potential.

Next, we calculate the lifetime of the $2p_{1/2}$ state using the experimental transition frequency of $2p \rightarrow 2s$, $\omega = 0.06791\text{au}$ in equation (8) of the task sheet. Since the $2s$ state is the only unoccupied lower state, this is the only transition that we need to consider. In doing this, we calculate a $2p_{1/2}$ lifetime of 19.0526ns – a value with an error of 29.7% from the experimental value of 27.102ns .

While this error is currently irreconcilable with our implementation of Green's approximation, we can consider first-order corrections to our obtained binding energies. To do this, we consider a correction of the form

$$\delta\varepsilon_a = \langle\delta V\rangle_a = \langle V_{e-e}\rangle_a - \langle V_{\text{Gr}}\rangle \quad (10)$$

where the subscript a corresponds to the valence state. The Green's term in equation (10) we evaluate with equation (18) of the task sheet. For the electron-electron term, $\langle V_{e-e}\rangle_a$, we evaluate according to equation (19) of the task sheet, introducing the Hartree screening function

$$y_{a,b}^k(r) \equiv \int_0^\infty P_a(r')P_b(r')\frac{r_{<}^k}{r_{>}^{k+1}}dr' \quad (11)$$

for which we utilise the supplied code `calculateYK.hpp`. The correction term relies on the radial wavefunction found for the respective state, and so it is calculated after forming the Hamiltonian and solving the Schrodinger equation.

Calculating the first-order corrections, we find $\delta\varepsilon_{2s} = -0.04786\text{au}$ and $\delta\varepsilon_{2p} = -0.00462\text{au}$. Adding these corrections onto our existing binding energies, $\varepsilon^{\text{corr}} = \varepsilon + \delta\varepsilon$, yields $\varepsilon_{2s}^{\text{corr.}} = -0.2037\text{au}$ (an error of -2.8% of the experimental value) and $\varepsilon_{2p}^{\text{corr.}} = -0.1300\text{au}$ (an error of 0.15% of the experimental value).

B3 - Self-consistent Hartree procedure

As a second step in refining our approach in approximating the experimental values, we use the Hartree procedure to obtain V_{Dir} ,

$$V_{\text{Dir}} = 2y_{1s,1s}^0(r) \quad (12)$$

which can be used in place of the Green's approximation in our Hamiltonian construction. To do this, we iteratively improve our best estimate of $P_{1s}(r)$ which is used in the Hartree screening function, beginning with a Hamiltonian that has no corrections. This procedure is shown in the following code block, where we return our 'converged' estimate of $P_{1s}(r)$ on a predetermined radial grid after solving the Schrodinger equation in `hartree_step()`.

```

1  std::vector<double> hartree_procedure(BSpline bspl, int N_red, std::vector<double> r){
2      // This function iteratively approximates the radial wavefunction for the 1s state using the
      Hartree procedure
3      std::cout << "Running Hartree procedure to convergence..." << std::endl;
4      Matrix matrix_H(N_red, N_red); // initialise our Hamiltonian in memory
5      Matrix matrix_B(N_red, N_red); // as above for the B matrix
6      populate_Hamiltonian(matrix_H, r, bspl, 0, &lithium_potential);
7      populate_B_Matrix(matrix_B, r, bspl);
8
9      MatrixAndVector matandvec = solveEigenSystem_AveBv(matrix_H, matrix_B, N_red);
10     std::vector<double> s_coeffs = get_expansion_coeffs(matandvec.mat, 0); // get the expansion
        coefficients from the eigenvectors
11     std::vector<double> s_Pr = vec_radial_wavefunction(s_coeffs, bspl, r); // calculate the
        radial wavefunction on our grid
12     double energy = matandvec.vec[0]; // get our first energy approximation
13     double err = 1e10; // start with arbitrarily high error
14
15     while (fabs(err) > 2.e-6){
16         matandvec = hartree_step(bspl, matrix_H, matrix_B, matandvec, r, s_Pr);
17         s_coeffs = get_expansion_coeffs(matandvec.mat, 0); // get the expansion coefficients from
            the eigenvectors
18         s_Pr = vec_radial_wavefunction(s_coeffs, bspl, r); // calculate the radial wavefunction
            on our grid
19
20         err = energy - matandvec.vec[0];
21         energy = matandvec.vec[0];
22     }
23     std::cout << "Hartree procedure converged!" << std::endl;
24     return s_Pr;
25 }

```

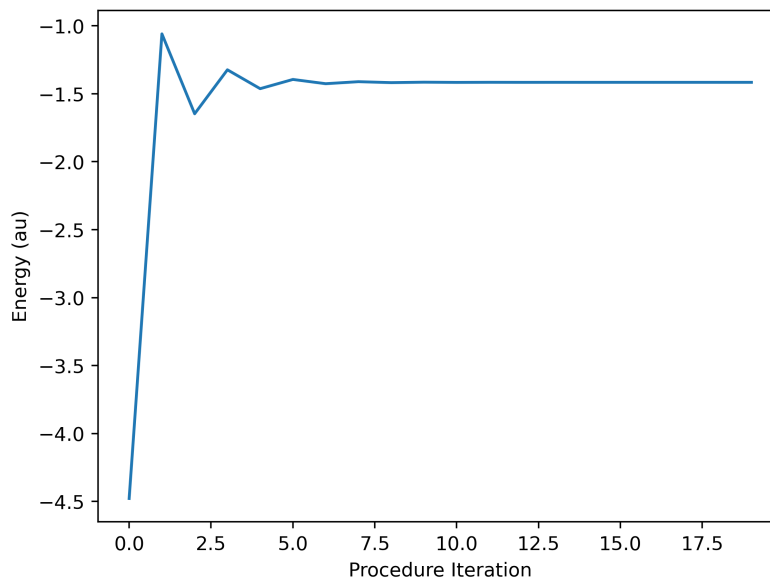


Figure. 3 The Hartree procedure eventually converges to a numerical solution for the 1s core state binding energy, beginning at the hydrogen-like potential on the first iteration.

After 8 or so iterations, we see very little oscillation about the limit value in Figure 3, where we reach $\lesssim 2 \times 10^{-6}$ au precision after 19 iterations. Using this potential and our converged value of $P_{1s}(r)$, we arrive at binding energies of $\varepsilon_{2s}^{\text{hartree}} = -0.182675$ au (7.8% error of the experimental value) and $\varepsilon_{2p}^{\text{hartree}} = -0.127073$ au (2.4% error of the experimental value). We see that this has much better agreement with the experimental value than the Green's approximation, but not quite as close as the first-order corrected Green's approximation. Where the Hartree procedure excels over the first-order correction is that we now have an approximation of the radial wavefunction for the 1s state, rather than just a correction term on the binding energy. This allows us to plot the radial probability densities (Figure 4) and infer the expected lifetime of the $2p_{1/2}$ state.

Using the same procedure as in B2, we calculate the $2p_{1/2}$ lifetime using the Hartree potential as 23.4975 ns. This is discrepant to the experimental value with an error of 13.3% – roughly half of the error associated with the same calculation using the Green's approximation.

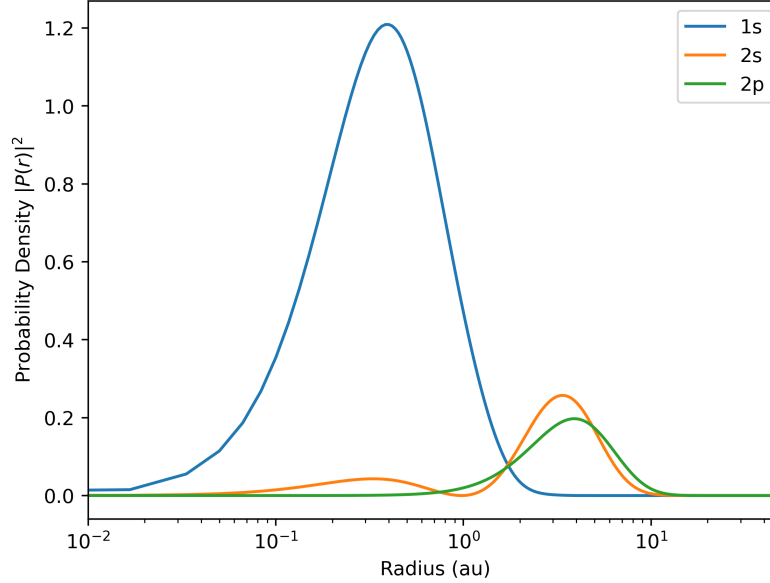


Figure. 4 Radial probability densities for the 1s and two first valence states, 2s and 2p, using the Hartree procedure.

B4 - Hartree-Fock

As a final and most complete approximation of lithium, we consider the full Hartree-Fock method which involves treating the energy exchange potential. To do this, our Hamiltonian matrix elements are populated as

$$H_{ij} = \frac{1}{2} \int b'_i(r) b'_j(r) dr + \int b_i(r) V_{\text{Dir}}(r) b_j(r) dr + \int b_i(r) V_{\text{exch}} b_j(r) dr \quad (13)$$

where

$$V_{\text{exch}} b_j(r) = -2\Lambda y_{1s, b_j}^k(r) P_{1s}(r) \quad (14)$$

As in the Hartree procedure, we begin with an initial guess of $P_{1s}(r)$ and iteratively update it until converged to a limiting value. Instead of beginning with a hydrogen-like potential here, though, we can begin with a (likely) better estimate that we'd calculated using the standard Hartree procedure. The iterative Hartree-Fock procedure is almost identical to that in the code block above (for the Hartree procedure) although with the aforementioned changes to the Hamiltonian construction.

With this new potential term, we see the 1s core state binding energy quickly decrease in Figure 5. Due to the 'good' initial guess of radial wavefunction, the Hartree-Fock procedure converges to the same precision in only 7 iterations compared to 19 with the Hartree procedure.

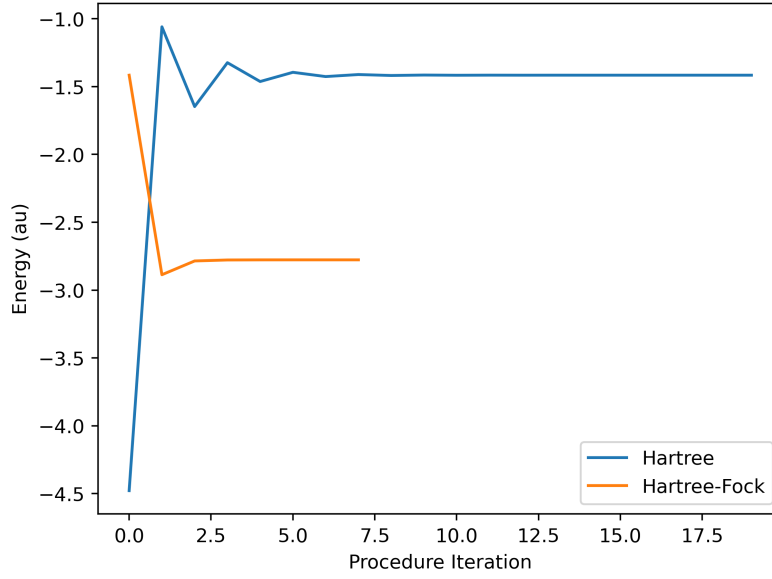


Figure. 5 The Hartree-Fock procedure quickly converges to a numerical solution for the $1s$ core state binding energy, beginning at the converged solution from the Hartree procedure after 19 iterations.

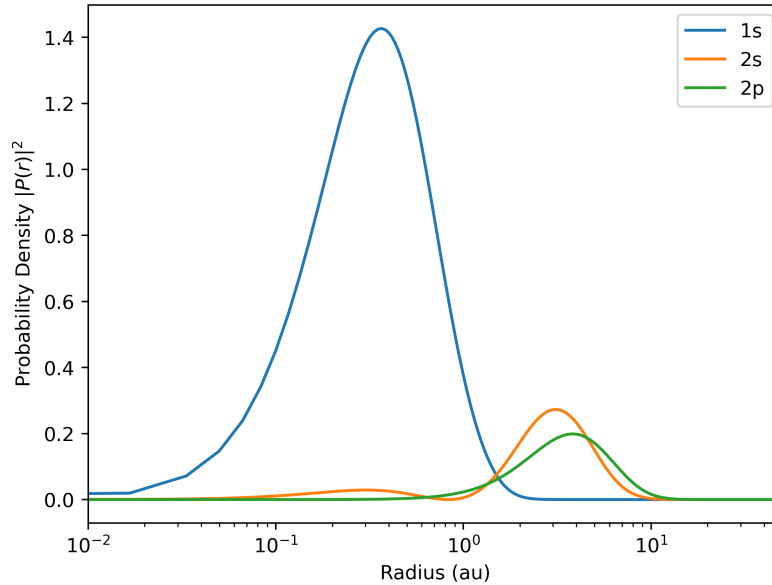


Figure. 6 Radial probability densities for the $1s$ and two first valence states, $2s$ and $2p$, using the full Hartree-Fock procedure.

With our final approximation converged, the binding energies for the first two valence states and the associated $2p_{1/2}$ lifetimes for all of our investigated procedures are shown in Table 2. We can see across our various plots of the probability densities that as our energy/lifetime estimates get more accurate, the valence state distribution peak shifts to higher radii, and the first bump of the $2s$ state gets smaller relative to the second bump.

Of course, we have made several assumptions/simplifications over the last 6 pages. To reduce the computation time, we reduced the number of grid points and the integration grid domain. In doing so, we've also assumed that the Hamiltonian integrals go to 0 for $r \rightarrow 0$, where we only go as low as 10^{-5} in our calculations. A more complete investigation would use a higher order integrator for these calculations, too, where we've employed the trapezoid rule. For Gaussians, the trapezoid rule tends to overestimate the area under the curve which would affect our results.

Method	2s Energy	2s Error	2p Energy	2p Error	2p _{1/2} Lifetime	2p _{1/2} Error
Experiment	-0.19814	-	-0.13023	-	27.102	-
Hydrogen-Like	-1.122	-466	-1.125	-761	-	-
Green's Approx.	-0.15582	21.36	-0.12541	3.70	19.5026	-29.7
Gr's First-order	-0.2037	-2.8	-0.1300	0.15	-	-
Hartree	-0.18265	7.8	-0.12707	2.4	23.4975	-13.14
Hartree-Fock	-0.19592	1.12	-0.12869	1.18	26.2601	-3.11

Table 2 First two valence state energies for our various approximations, and their associated 2p_{1/2} lifetimes with errors. All energy values are in atomic units (au), lifetimes in nanoseconds, and errors in % from the experimental value.

Our treatment of the basis functions involved calculating 50 7th order B-splines – a more rigorous approach may be to consider *more*, physically motivated basis functions such as hydrogen-like wavefunctions. Furthermore, or Hartree and Hartree-Fock procedures involved iterating only over the $P_{1s}(r)$ radial wavefunction; in reality, we might need to consider the convergence of the radial wavefunctions of all of the states we investigate (especially in the Hartree-Fock case). In our calculation of the 2p_{1/2} lifetimes, we've also assumed the experimental transition frequency but this also depends on the energies and wavefunctions involved, and so we may be underestimating our error of these values.

Conclusion

In summary, we've considered approximate treatments of the atomic physics of lithium in increasing levels of complexity and accuracy. Naturally, the most complete method considered, the Hartree-Fock, gave the most accurate energy and lifetime values compared to experimentally obtained estimates. All of our methods were not without error, however, and we briefly discussed obvious points of error with some possible ways to reduce this.